

Comparison of Models of Critical Opacity in the Quark-Gluon Plasma

Xiangdong Li

Department of Computer System Technology

New York City College of Technology of the City University of New York

Brooklyn, New York 11201

C. M. Shakin*

Department of Physics and Center for Nuclear Theory

Brooklyn College of the City University of New York

Brooklyn, New York 11210

(Dated: July, 2004)

Abstract

In this work we discuss two methods of calculation of quark propagation in the quark-gluon plasma. Both methods make use of the Nambu-Jona-Lasinio model. The essential difference of these calculations is the treatment of deconfinement. A model of confinement is not included in the work of Gastineau, Blanquier and Aichelin [hep-ph/0404207], however, the meson states they consider are still bound for temperatures greater than the deconfinement temperature T_c . On the other hand, our model deals with unconfined quarks and includes a description of the $q\bar{q}$ resonances found in lattice QCD studies that make use of the maximum entropy method (MEM). We compare the $q\bar{q}$ cross sections calculated in these models.

PACS numbers: 12.39.Fe, 12.38.Aw, 14.65.Bt

*email address:casbc@cunyvm.cuny.edu

It is found in studies of heavy-ion interactions at RHIC that the system very rapidly reaches equilibrium and that a model based upon hydrodynamics is appropriate for the early stages of the collision in which one expects to form a quark-gluon plasma [1]. Recently, Gastineau, Blanquier and Aichelin have proposed a model of critical opacity based upon their calculation of the $q\bar{q}$ interaction for temperatures in the range of 0 to 350 MeV [2]. A central feature of their model is the temperature dependence of masses of the u , d and s quarks, as well as the masses of the π and K mesons. (See Fig. 1 of Ref. [2].) In their model of the $q\bar{q}$ scattering amplitude they calculate s , t and u -channel exchange of π and K mesons in the temperature range $0 < T < 350$ MeV. (We remark that deconfinement takes place at $T_c \sim 170$ MeV in unquenched QCD calculations and at $T_c = 270$ MeV in quenched calculations.) In Ref. [2], the matrix elements in the s and t channels are given by

$$\begin{aligned} -i\mathcal{M}_t = & \delta_{c_1,c_3}\delta_{c_2,c_4}\bar{u}(p_3)Tu(p_1)[i\mathcal{D}_t^S(p_1 - p_3)]v(p_4)T\bar{v}(p_2) \\ & + \delta_{c_1,c_3}\delta_{c_2,c_4}\bar{u}(p_3)(i\gamma_5 T)u(p_1)[i\mathcal{D}_t^P(p_1 - p_3)]v(p_4)(i\gamma_5 T)\bar{v}(p_2) \end{aligned} \quad (1)$$

$$\begin{aligned} -i\mathcal{M}_s = & \delta_{c_1,c_2}\delta_{c_3,c_4}\bar{v}(p_2)Tu(p_1)[i\mathcal{D}_s^S(p_1 + p_2)]v(p_4)T\bar{u}(p_3) \\ & + \delta_{c_1,c_2}\delta_{c_3,c_4}\bar{v}(p_2)(i\gamma_5 T)u(p_1)[i\mathcal{D}_s^P(p_1 + p_2)]v(p_4)(i\gamma_5 T)\bar{u}(p_3), \end{aligned} \quad (2)$$

where $p_1(p_2)$ is the momentum of the incoming $q(\bar{q})$ and $p_3(p_4)$ that of the outgoing $q(\bar{q})$. The c_i are color indices and the various T 's are the isospin projectors on the meson states. Here, \mathcal{D}^S and \mathcal{D}^P are the meson propagators of the form obtained in the NJL model,

$$\mathcal{D}^S = \frac{G_S}{1 - G_S J^S} \quad (3)$$

and

$$\mathcal{D}^P = \frac{G_P}{1 - G_P J^P}, \quad (4)$$

with J^S and J^P being the polarization tensors in the scalar and pseudoscalar channels, respectively. (In Eqs. (3) and (4) we have modified the notation of Ref. [2] to be in closer correspondance to the notation we have used in our work.)

In Ref. [2] the following Lagrangian is used without the term proportional to G_V

$$\begin{aligned}
\mathcal{L} = & \bar{q}(i\gamma\!/\! - m^0)q + \frac{G_S}{2} \sum_{i=0}^8 [(\bar{q}\lambda^i q)^2 + (\bar{q}i\gamma_5\lambda^i q)^2] \\
& - \frac{G_V}{2} \sum_{i=0}^8 [(\bar{q}\lambda^i\gamma_\mu q)^2 + (\bar{q}\lambda^i\gamma_5\gamma_\mu q)^2] \\
& + \frac{G_D}{2} \{\det[\bar{q}(1 + \lambda_5)q] + \det[\bar{q}(1 - \lambda_5)q]\}.
\end{aligned} \tag{5}$$

Here, m^0 is a current quark mass matrix, $m^0 = \text{diag}(m_u^0, m_d^0, m_s^0)$. The λ_i are the Gell-Mann (flavor) matrices and $\lambda^0 = \sqrt{2/3}\mathbf{1}$, with $\mathbf{1}$ being the unit matrix. The fourth term is the 't Hooft interaction. [Note that in the notation used in Ref. [2], G_S and G_V replace $G_S/2$ and $G_V/2$ of Eq. (5).]

In order to make contract with the results of lattice simulations [3-6] we use the model with the number of flavors, $N_f = 1$. Therefore, the λ^i matrices in Eq. (5) may be replaced by unity. We then have used

$$\begin{aligned}
\mathcal{L} = & \bar{q}(i\gamma\!/\! - m^0)q + \frac{G_S}{2}[(\bar{q}q)^2 + (\bar{q}i\gamma_5q)^2] \\
& - \frac{G_V}{2}[(\bar{q}\gamma_\mu q)^2 + (\bar{q}\gamma_5\gamma_\mu q)^2]
\end{aligned} \tag{6}$$

in order to calculate the hadronic current correlation functions in earlier work [7-9]. Spectral functions obtained using lattice QCD and MEM are shown in Fig. 1 and 2 [3].

We note that the unpolarized total cross section for a resonance of mass m_R in the s -channel may be written

$$\sigma_{tot} = \frac{1}{3\pi} E^2 \frac{g^4}{(P^2 - m_R^2)^2 + m_R^2 \Gamma_R^2}, \tag{7}$$

where $s = 4E^2$ in the center-of-mass. The more general result is obtained by using the expression

$$\frac{G_S}{1 - G_S J(P^2)} \simeq -\frac{g^2}{P^2 - m_R^2 + im_R \Gamma_R}, \tag{8}$$

so that Eq. (7) becomes

$$\sigma_{tot} = \frac{N}{3\pi} E^2 \left| \frac{G_S}{1 - G_S J(P^2)} \right|^2 \tag{9}$$

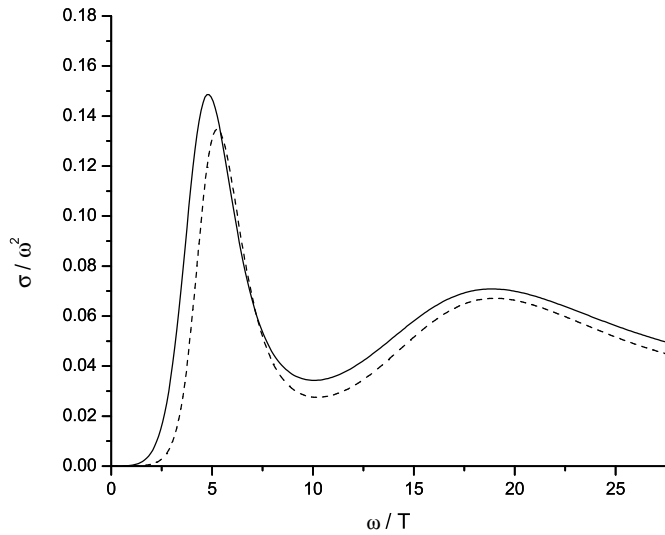


FIG. 1: The spectral functions σ/ω^2 for pseudoscalar states obtained by MEM are shown [3]. The solid line is for $T/T_c = 1.5$ and the dashed line is for $T/T_c = 3.0$. The second peak is lattice artifact [3].

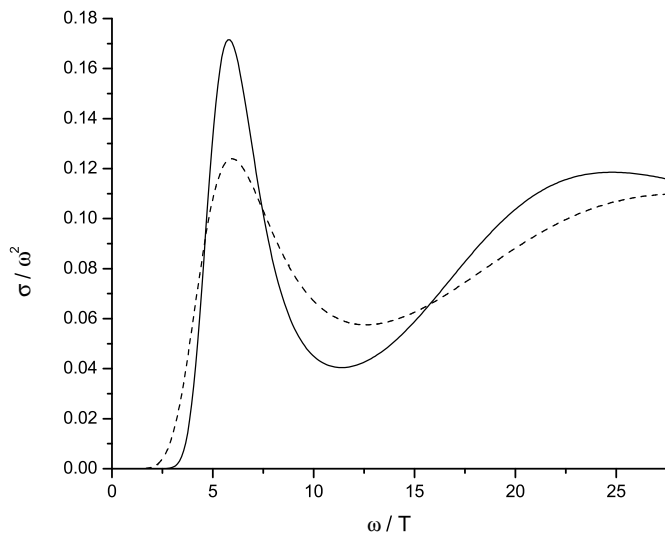


FIG. 2: The spectral functions σ/ω^2 for vector states obtained by MEM are shown [3]. See the caption of Fig. 1. The second peak is lattice artifact [3].

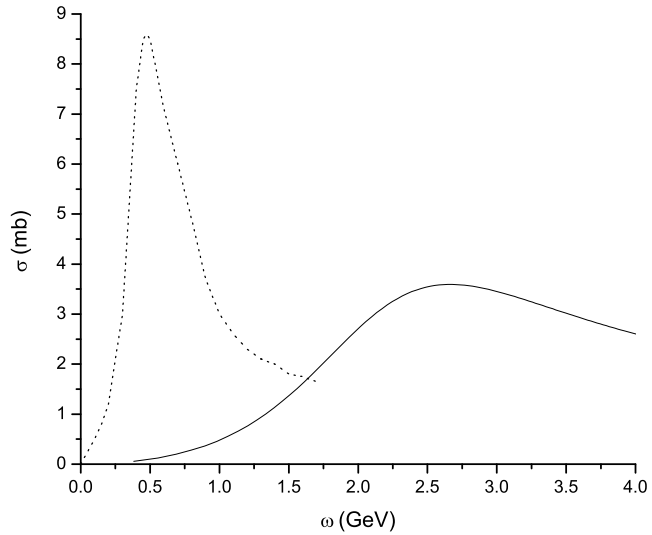


FIG. 3: The dotted line shown the result for $T = 350$ MeV obtained in Ref. [2]. (See Fig. 3 of Ref. [2] for this result and for results at other temperatures.) The solid curve presents the results calculated using our model at $T = 350$ MeV [7-9].

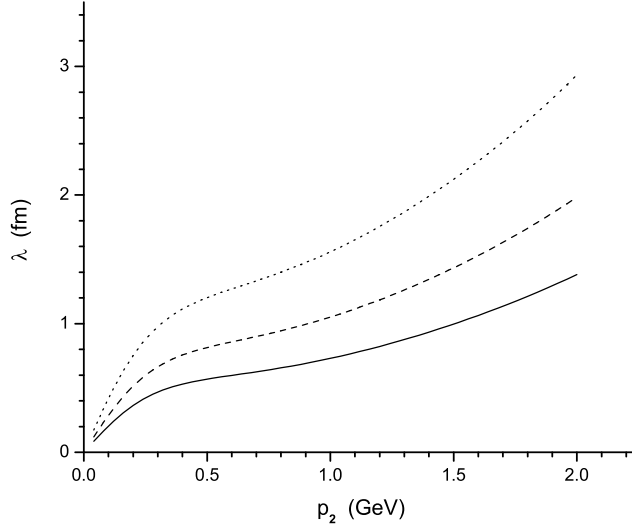


FIG. 4: Quark mean-free path, $\lambda(p_2)$, shown for different densities of antiquarks as a function of the quark momentum p_2 . (See Ref. [10] and Eq. (8) of the present work for the parametrization of the antiquark densities used in our calculation.) Here, $\mu = 1.1$ GeV (dotted curve), $\mu = 1.3$ GeV (dashed curve) and $\mu = 1.5$ GeV (solid curve).

where N is a statistical factor which we take to be $N = \sum_J (2J + 1) = 8$, since we consider a sum over scalar, pseudoscalar, vector and axial-vector resonances in our model. The calculation of $J(P^2)$ is discussed in great detail in our earlier work [7-9] and we do not repeat that discussion here. (In that work we have used a Gaussian regulator rather than the sharp cutoff usually used in the case of the NJL model.)

The result for the cross section $u + \bar{u} \rightarrow u + \bar{u}$ obtained in Ref. [2] is shown as a dotted line in Fig. 3. The solid line shows the result obtained in our model [7-9].

The application of our model to calculate the quark mean-free path is described in Ref. [10] and some results are shown in Fig. 4 for different densities of antiquarks in the plasma [10]. That distribution is parametrized as in Eq. (2.7) of Ref. [10] with

$$n(\vec{p}_1) = \frac{1}{\exp \beta [E(\vec{p}_1) - \mu] + 1}, \quad (10)$$

$\beta = 1/T$ and $E(\vec{p}_1) = [\vec{p}_1^2 + m^2]^{1/2}$. (See the caption of Fig. 4.)

The main difference between our model and that of Ref. [2] is that we recognize that the system is deconfined above the critical temperature. The resonances calculated in Ref. [2] using the NJL model that play the major role in the results of that work are not present in the deconfined plasma. In our work we have used the resonances found in the deconfined phase when using lattice QCD and the maximum entropy method. Our work is closer in spirit to that of the Stony Brook group [11-13] who also make reference to the QCD lattice data in their discussion of the quite small quark mean-free paths.

-
- [1] P. F. Kolb and V. Heinz, nucl-th/0305084.
- [2] F. Gastineau, E. Blanquier, and J. Aichelin, hep-ph/0404207.
- [3] P. Petreczky, J. Phys. G **30**, S431-S440 (2004); hep-ph/0305189 and private communication.
- [4] I. Wetzorke, F. Karsch, E. Laermann, P. Petreczky, and S. Stickan, Nucl. Phys. B (Proc. Suppl.) **106**, 510 (2002)
- [5] F. Karsch, S. Datta, E. Laermann, P. Petreczky, and S. Stickan, and I. Wetzorke, Nucl. Phys. A **715**, 701c (2003)

- [6] F. Karsch, E. Laermann, P. Petreczky, S. Stickan, and I. Wetzorke, Phys. Lett. B **530**, 147 (2002).
- [7] Bing He, Hu Li, C. M. Shakin, and Qing Sun, Phys. Rev. D **67**, 014022 (2003).
- [8] Bing He, Hu Li, C. M. Shakin, and Qing Sun, Phys. Rev. D **67**, 114012 (2003).
- [9] Bing He, Hu Li, C. M. Shakin, and Qing Sun, Phys. Rev. C **67**, 065203 (2003).
- [10] Xiangdong Li, Hu Li, C. M. Shakin, and Qing Sun, Phys. Rev. C **69**, 065201 (2004).
- [11] E. Shuryak, Prog. Part. Nucl. Phys. **53**, 273 (2004).
- [12] G. E. Brown, C. H. Lee, M. Rho, and E. Shuryak, hep-ph/0312175
- [13] G. E. Brown, C. H. Lee, M. Rho, and E. Shuryak, hep-ph/0402068; G. E. Brown, C. H. Lee, and M. Rho, hep-ph/0402207.